Journal Pre-proof

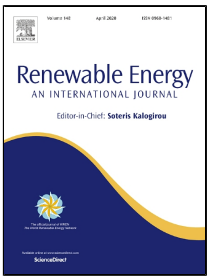

Optimization and performance analysis of a solar concentrated photovoltaic-thermoelectric (CPV-TE) hybrid system

Oussama Rejeb, Samson Shittu, Chaouki Ghenai, Guiqiang Li, Xudong Zhao, Maamar Bettayeb

PII:	S0960-1481(20)30187-7
DOI:	https://doi.org/10.1016/j.renene.2020.02.007
Reference:	RENE 13028
To appear in:	*Renewable Energy*
Received Date:	01 August 2019
Accepted Date:	03 February 2020

Please cite this article as: Oussama Rejeb, Samson Shittu, Chaouki Ghenai, Guiqiang Li, Xudong Zhao, Maamar Bettayeb, Optimization and performance analysis of a solar concentrated photovoltaic-thermoelectric (CPV-TE) hybrid system, *Renewable Energy* (2020), https://doi.org/10.1016/j.renene.2020.02.007

Optimization and performance analysis of a solar concentrated photovoltaic-thermoelectric (CPV-TE) hybrid system

Oussama Rejeb [a], Samson Shittu [b], Chaouki Ghenai [c], Guiqiang Li [b], Xudong Zhao [b], Maamar Bettayeb [d,e]

a. Sustainable Energy Development Research Group, Research Institute for Science and Engineering (RISE), University of Sharjah, P.O. Box 27272, Sharjah, United Arab Emirates.
b. Research Centre for Sustainable Energy Technologies, University of Hull, HU6 7RX, United Kingdom
c. Department of Sustainable and Renewable Energy Engineering, College of Engineering, University of Sharjah, Sharjah, United Arab Emirates.
d. Department of Electrical Engineering, University of Sharjah, Sharjah, United Arab Emirates.
e. Center of Excellence in Intelligent Engineering Systems (CEIES), King Abdulaziz University, Jeddah, Saudi Arabia

ABSTRACT

This work presents, for the first time, a statistical model to forecast the electrical efficiency of concentrated photovoltaic-thermoelectric system (CPV-TE). The main objective of this work is to analyze the impact of the input factors (product of solar radiation and optical concentration, external load resistance, leg height of TE and ambient temperature) most affecting the electrical efficiency of CPV-TE system. An innovative and integrated approach based on a multi-physics numerical model coupling radiative, conductive and convective heat transfers Seebeck and photoelectrical conversion physical phenomena inside the CPV-TE collector and a response surface methodology (RSM) model was developed. COMSOL 5.4 Multiphysics software is used to perform the three-dimensional numerical study based on finite element method. Furthermore, results from the numerical model is then analysed using the statistical tool, response surface methodology. The analysis of variance (ANOVA) is conducted to develop the quadratic regression model and examine the statistical significance of each input factor. The results reveal that the obtained determination coefficient (R^2) for electrical efficiency is 0.9945. An excellent fitting is achieved between forecast values obtained from the statistical model and the numerical data provided by the three-dimensional numerical model. The influence of the parameters in order of importance on the electrical efficiency are respectively: product of solar radiation and optical concentration, the height legs of TE, external electrical resistance load, and ambient temperature. A simple polynomial statistical model is created in this work to predict and maximize the electrical efficiency from the solar CPV-TE system based on the four investigated input parameters. The maximum electrical efficiency of the proposed CPVTE (17.448%) is obtained for optimum operating parameters at 229.698 W/m² value of product of solar radiation and optical concentration, 303.353 K value of ambient temperature, 2.681Ω value of resistance electrical load and at 3.083 mm value of height of TE module.

Keywords: Concentrated photovoltaic-thermoelectric system (CPV-TE) ; Response surface methodology (RSM); Electrical efficiency enhancement

Nomenclature

A_{te}	Area of TE top surface, m^2	κ	Thermal conductivity, $W/m \cdot K$
C	Concentration ratio	ρ	Density, kg/m^3
C_P	Specific heat capacity, $J/kg \cdot K$	β	PV temperature coefficient, $1/K$
G	Solar irradiance, W/m^2	***Abbreviations***	
h	Heat transfer coefficient, $W/m^2 \cdot K$	ANN	Artificial neural network
I	Current, A	Bi_2Te_3	Bismuth telluride
P_{teg}	TEG power output, W	CPV-TE	Concentrated photovoltaic-thermoelectric
$\dot{q}_i$	Volumetric energy absorption, W/m^3	EVA	Ethylene vinyl acetate
Q_h	Input heat flux, W/m^2	PV	Photovoltaic
R_{in}	Internal resistance, Ω	PV-TE	Photovoltaic-thermoelectric
R_L	Load resistance, Ω	RSM	Response surface methodology
T	Temperature, K	TE	Thermoelectric

V_{OC}	Open circuit voltage, V	TEG	Thermoelectric generator
Z	Figure of merit, $1/K$	TPT	Tedlar polyester tedlar
Greek symbols		***Subscripts***	
α	Seebeck coefficient, V/K	amb	Ambient
η	Efficiency, %	pv	Photovoltaic cell
σ	Electrical conductivity, S/m	sky	Sky

1. INTRODUCTION

The increase in global demand for energy, scarcity of fossil energy resources and climate change are undeniable realities. Therefore, there is an urgent need for the development of clean energy sources that are renewable and cost-effective to decrease fossil fuel reliance and consequently, carbon emissions. The sun is an abundant and ecological source of renewable energy. Solar energy can be utilized by converting it into two harnessed forms including electricity and thermal energy. Through the photovoltaic effect, the photovoltaic (PV) module can convert sunlight into electrical energy. However, the absorbed sunlight and heat dissipated from the solar cells lead to an increase in its temperature. Therefore, thermal management techniques for photovoltaic systems have attracted many interests in recent years [1–5]. Several approaches to regulate the PV temperature have been considered including air-cooling, water-cooling, heat pipes, phase change materials and thermoelectric cooling. A thermoelectric generator (TE) is a solid-state device that transforms a temperature difference into an electric current. It consists of several pairs of different semiconductor materials (p-type, n-type) inserted between two ceramic plates thermally connected in parallel and electrically in series [6]. The advantages of a TE include simple design, small size, absence of any moving part, high reliability and zero emission [7]. However, low efficiency and high cost of material are the two main disadvantages of the TE which have hindered its full spread application [8]. Coupling a TE with a PV will allow for the utilization of the waste heat from the PV for supplementary energy generation while simultaneously cooling the PV for better overall performance [9].

Van Sark [10] developed an analytical model of a PV-TE system to study the possibility of integrating thermoelectric modules into a photovoltaic module. Their results indicate that a 11% enhancement in electrical output is obtained compared to a conventional one under Malaga climatic conditions. Lekbir et al. [11] performed an experimental study on a PV-TE system and found that the hybrid system produced a higher maximum power output compared to the

individual PV and TEG. Rodrigo et al. [12] studied the performance of a passively cooled hybrid concentrated PV-TE and results showed that passive cooling improves the performance of the hybrid system. Furthermore, Lorenzi et al. [13] investigated the theoretical efficiency of a hybrid PV-TE and found that the hybrid system's effectiveness was 4-5 % greater than that of the PV alone. Optimizing the performance of a PV-TE is essential to obtain improved performance [14–16]. In particular, geometry optimization of a TE in a PV-TE significantly affects the hybrid system performance. Hashim et al. [17] presented a numerical study on a TE geometry optimization in a hybrid PV-TE. Results obtained showed that the TE geometry affects the operating temperature of the PV and consequently, the overall performance of the hybrid system. Li et al. [18] presented a comparative study on the optimum thermoelectric (TE) geometry in a PV-TE. Results showed that the geometry of the TE in the hybrid PV-TE significantly affects the overall performance.

The physical phenomena governing the electrical and thermal behaviour of PV-TE are numerous and complex. In this regard, an analytical model describing its performance gives a low precision compared to the numerical method. For this, it is necessary to develop a numerical model using discretization schemes, to study the mechanisms of heat transfer (heat diffusion, thermal radiation, mass transfer energy transport), the mechanisms of photovoltaic conversion, and the phenomena induced in thermoelectricity via the Seebeck effect (energy generation by temperature gradient). In the literature, different discretization schemes were used, such as the finite difference method (FDM), finite element method (FEM), and finite volume method (FVM). Due to the diversity of the physical phenomena inside our PV-TE, as well as, the coupling between the energy equation and the continuity equation of the electric charge, finite difference method based on the approximation of a Taylor series, will not be able to provide a solution with higher accuracy. For this reason, integral methods, namely FVM and FEM, are the most effective techniques used to solve the mathematical model with satisfactory precision. The FEM has been adopted to solve a two-dimensional PV-TE unsteady-state model [19]. Their results show that a 5.06 % improvement in electrical output is achieved compared to a conventional one under Shiraz (Iran) climatic conditions. Shittu et al. [20] performed a detailed comparative study on the performance of a concentrated PV-TE with and without a flat plate heat pipe. COMSOL Multiphysics software, which is based on the FEM, was used for the numerical investigation and results showed that the additional heat pipe to the hybrid PV-TE significantly improves the performance of the system. Furthermore, Mahmoudinezhad et al. [21] presented an experimental and numerical study of a transient PV-TE. The numerical study was performed using COMSOL, and the results obtained showed that the TEG could assist in stabilizing the power output of the hybrid system under different weather conditions. Nevertheless, this type of numerical modelling requires the knowledge of heat transfer phenomena (radiation, convection, conduction) inside the CPV-TE. Besides, the comprehension of the photovoltaic conversion and the Seebeck effect mechanisms, the excellent choice of the boundary condition used in discretization procedures, which need a considerable resolution time, particularly for fine meshes are required. Moreover, using the numerical method, the determination of parameters affecting the electrical efficiency is

performed by studying the effect of only one factor at a time; it neglects the combined interactions between parameters. Therefore, this type of modelling is not able to investigate the impact of the parameter most influencing on the efficiency of the PV-TE compared to other parameters.

To avoid this gap, the optimization of analytical procedures can be implemented as artificial neural networks (ANN). The response surface methodology (RSM) can also solve this problem. In fact, the benefits of this method (RSM) is the ability to obtain the maximum information from limited trials compared to ANN and Genetic algorithm (GA).

To the extent of the authors' knowledge, this is the first type of parametric study on the effects of the most important parameters influencing the electrical efficiency of the CPV-TE. This study focuses more on the combined interactions between the four input factors (the product of the solar radiation and optical concentration, external load resistance, leg height of TE and ambient temperature). Another novelty of the present study is the development of new quadratic equation to forecast the electrical efficiency of the concentrated photovoltaic-thermoelectric (CPV-TE) system based on the considered input parameters. The impact of the most critical parameters affecting the efficiency of CPV-TE system is also determined as well as the optimum parameters for obtaining the maximum electrical efficiency of the proposed CPV-TE collector.

The rest of this work is constructed as follows; section 2 presents a three-dimensional mathematical model governing the physical phenomenon inside the CPV-TE and a detailed statistical model. Section 3 examines an analysis of variance and a comparison, model estimation. Finally, the results are analysed in Section 4 and the conclusion extracted from this work is presented in Section 5.

2. Numerical Model

2.1. Three-Dimensional Mathematical Model

The schematic diagram of our considered CPV-TE is presented in Fig.1, and its optical and thermos-physical properties are summarized in Table 1. The photovoltaic module consists of five different layers, i.e., glazing, upper and bottom of EVA (Ethylene Vinyl Acetate), silicon solar cell and TPT back sheet layers. The silicon layer is sandwiched between the EVA, and all the PV layers are of equal dimension and in direct contact. The bismuth telluride (Bi_2Te_3) thermoelectric modules are thermally attached to the TPT (Tedlar- Polyester-Tedlar) backside. In this present work, a commercial thermoelectric generator (GM250-71-14-16) consisting of 71 pairs of different semiconductor materials (p-type and n-type) connected

electrically in series with copper electrodes and inserted between two ceramic plates is used. Temperature dependent Bismuth telluride (Bi_2Te_3) thermoelectric material properties are used in this study which are obtained from [22] and the remaining material properties used are obtained from [20]. Compared to the conventional photovoltaic module, the advantage of the coupling the PV module with thermoelectric modules is to maintain the solar cells operating temperatures at the satisfactory level favouring a good photovoltaic conversion efficiency, as well as, to recover the maximum heat loss from these cells in order to transform it into additional electricity power (the Seebeck effect). The PV and TE have the same dimensions (40 mm x 40 mm) and the geometric parameters are shown in Table 2. The boundary conditions and assumptions considered in this study are given as:

1) Heat loss via convection and radiation is considered at the glass upper surface of the PV
2) Initial temperature is assumed equal to the ambient temperature
3) Considering radiative heat loss, the front surface of the PV is taken to view the sky
4) Solar cell efficiency is assumed to be 17 % at 298.15 K and temperature coefficient of 0.0045 1/K [20]
5) Thermoelectric thermal and electrical contact resistances are ignored
6) Adiabatic condition is assumed on the surfaces of the TE
7) A fixed temperature of 293.15 K is assumed at the cold side of the TEG.

Table 1: Optical properties of PV [23]**.**

Material	**Reflectivity**	**Absorptivity**	**Transmissivity**	**Emissivity**
Glass	0.04	0.04	0.92	0.85
EVA	0.02	0.08	0.9	
Polycrystalline silicon	0.08	0.9	0.02	
TPT	0.86	0.128	0.012	0.92

Table 2: CPV-TE geometric parameters [18,21]

Parameter	**Value**
Photovoltaic (PV)	
Area	$30\ mm \times 30\ mm$
Glass height	$3.20\ mm$
EVA height	$0.46\ mm$

Silicon height	0.18 mm
Tedlar height	0.18 mm
Thermoelectric generator (TEG)	
Area	30 mm × 30 mm
Leg area	1 mm × 1 mm
Copper height	0.3 mm
Ceramic height	0.8 mm

Based on Fourier's law, the transient temperature within the PV module is presented by the three-dimensional heat conduction for every solid layer in the photovoltaic module and is given by the following equation:

$$\rho_i C_{p,i} \frac{\partial T_{i\,(x,y,z)}}{\partial t} = k_i\left(\frac{\partial^{2T_i}(x,y,z)}{\partial x^2} + \frac{\partial^{2T_i}(x,y,z)}{\partial y^2} + \frac{\partial^{2T_i}(x,y,z)}{\partial z^2}\right) + q_i \quad \text{and} \quad i=1,2,3,4,5 \tag{1}$$

where q_i represent heat generation per unit volume, ρ_i,$C_{p,i}$ and k_i designate the specific heat, density and thermal conductivity, respectively, of each solid layer in the photovoltaic module. In this current investigation, the value of i varies from 1 to 5 for glass; above EVA, polycrystalline silicon solar cell, above EVA, and the Tedlar layers, respectively.

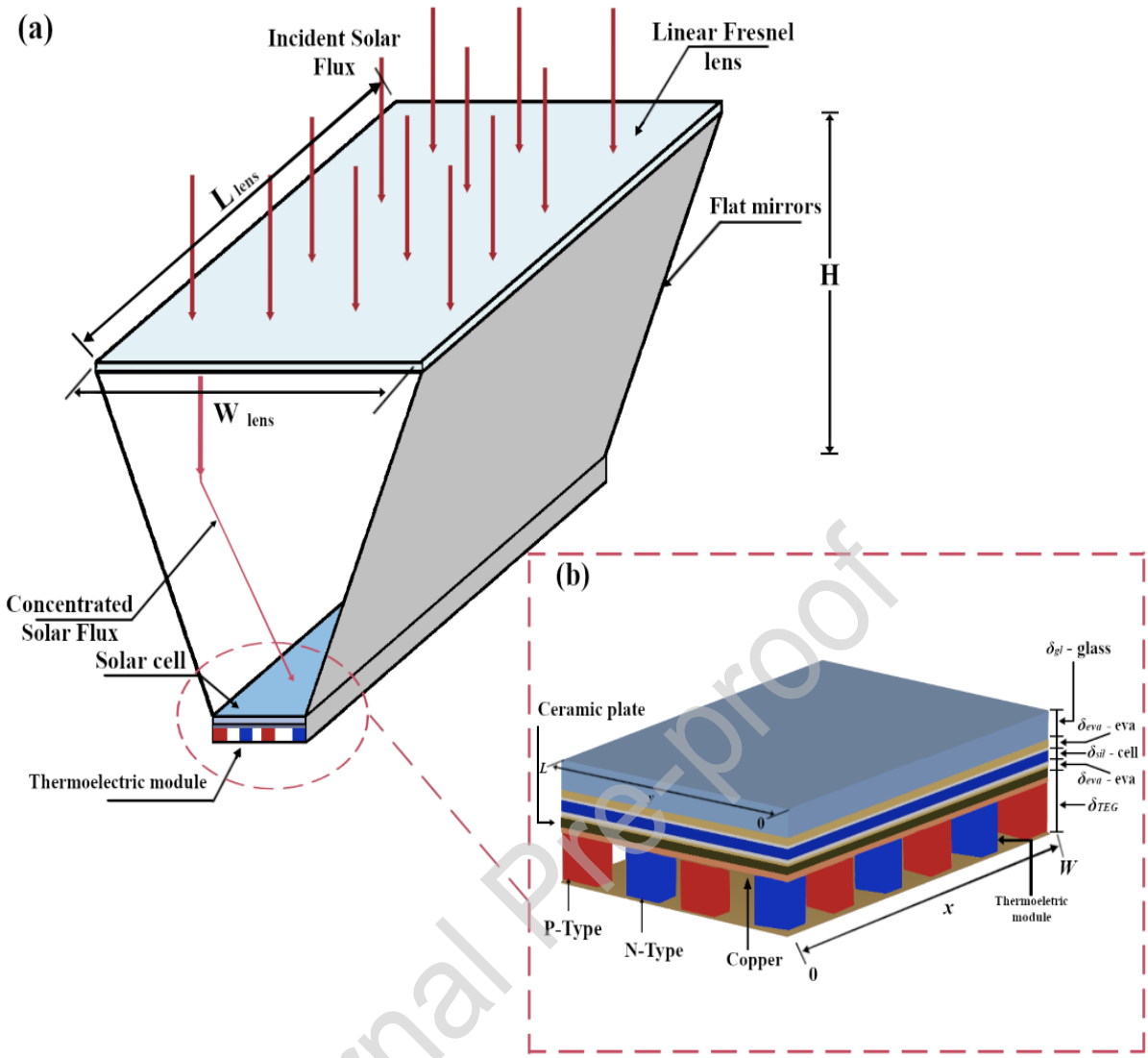

Figure 1: CPV-TE system considered in the present study

The volumetric solar energy absorption can be estimated as follows [20]:

$$\dot{q}_i = \frac{(1-\eta_{pv})G_{rec,i} \times \alpha_i \times A_i \times C}{V_i} \quad (2)$$

where $A_i, V_i, \rho_i, \alpha_i$ are the surface, volume, reflectivity and absorptivity of each solid layer respectively, C denotes the solar concentration ratio.

The 3 D dimensional steady state TEG model developed in this work involves the energy equation and electric potential equation, which are determined by the following expression:

The Conservation of energy can be rewritten as:

$$\rho C_p \frac{\partial T}{\partial t} + \nabla \cdot \vec{q} = \dot{q} \quad (3)$$

where $\dot{q}$ represent the heat generation per unit volume, C_p,ρ designate the specific heat, respectively. $\vec{q}$ is the heat flux vector

The electric charge continuity equation can be written as:

$$\nabla \cdot \left(\vec{j} + \frac{\partial \vec{D}}{\partial t}\right) = 0 \quad (4)$$

where $\vec{D}$ designates the electric flux density vector, $\vec{j}$ represents the electric current density vector

The coupled thermoelectric governing equations can be written as :

$$\nabla \cdot \left(T\alpha\vec{J}\right) - \nabla \cdot (k\nabla \mathrm{T}) = \dot{q} \quad (5)$$

$$\nabla \cdot (\sigma\alpha\nabla \mathrm{T}) + \nabla \cdot (\sigma\nabla\varphi) = 0 \quad (6)$$

where α represents the Seebeck coefficient, σ designates the electrical conductivity.

- **Boundary conditions**

The boundary conditions, the temperature variation in the different points of the system and their conditions have been detailed in the revised version as shown below:

To solve the heat partial differential equation, the boundary conditions must be adopted. First, for the upper side of the PV panel at $0 \le x \le \mathrm{W}$, $0 \le y \le \mathrm{L}$ and $z = \delta_{gl} + 2\delta_{eva} + \delta_{cel} + \delta_{TPT} + \delta_{TEG}$, a combination between radiation and convective heat exchanges are considered, and can be represented as follows:

$$k_{glass}\frac{\partial T_{glass}}{\partial z} = \alpha_{glass}G_T + h_{wind}(T_{amb} - T_{glass}) + h_{rad}(T_{sky} - T_{glass}) \quad (7)$$

For the glass- top side of Ethylene vinyl acetate (EVA) interface at $0 \le x \le \mathrm{W}$, $0 \le y \le \mathrm{L}$ and $z = \delta_{eva,top} + \delta_{cel} + \delta_{eva,bottom} + \delta_{TPT} + \delta_{TEG}$, conductive heat transfer boundary condition is given as follows:

$$k_{glass}\nabla \mathrm{T}_{glass} = k_{eva,top}\nabla \mathrm{T}_{eva,top} \quad (8)$$

For the top side of Ethylene vinyl acetate (EVA) - Solar cell interface at $0 \leq x \leq \mathrm{W}$, $0 \leq y \leq \mathrm{L}$, $z = \delta_{cel} + \delta_{eva,bottom} + \delta_{TPT} + \delta_{TEG}$conductive heat transfer boundary condition is estimated as follows:

$$k_{cel}\nabla \mathrm{T}_{cel} = k_{eva,top}\nabla \mathrm{T}_{eva,top} \quad (9)$$

For the solar cell- bottom side of Ethylene vinyl acetate (EVA) interface at $0 \leq x \leq \mathrm{W}$, $0 \leq y \leq \mathrm{L}$ and $z = \delta_{eva,bottom} + \delta_{TPT} + \delta_{TEG}$, conductive heat transfer boundaries conditions is determined as follows:

$$k_{cel}\nabla \mathrm{T}_{cel} = k_{eva,bottom}\nabla \mathrm{T}_{eva,bottom} \quad (10)$$

For the bottom side of Ethylene vinyl acetate (EVA) - Tedlar interface at $0 \leq x \leq \mathrm{W}$, $0 \leq y \leq \mathrm{L}$ and $z = \delta_{TPT} + \delta_{TEG}$, the conductive heat transfer boundary condition is given as follows:

$$k_{eva,bottom}\nabla \mathrm{T}_{eva,bottom} = k_{Tedlar}\nabla \mathrm{T}_{Tedlar} \quad (11)$$

For the bottom side of the PV panel-Thermoelectric module interface at $0 \leq x \leq \mathrm{W}$, $0 \leq y \leq \mathrm{L}$ and $z = \delta_{TEG}$, a conductive heat transfer boundary condition is adopted, and is given by the following equation:

$$k_{c,TEG}\nabla \mathrm{T}_{c,TEG} = k_{Tedlar}\nabla \mathrm{T}_{Tedlar} \quad (12)$$

For the bottom side of the CPV-TE collector at $0 \leq x \leq \mathrm{W}$, $0 \leq y \leq \mathrm{L}$ and $z = 0$, a convective heat exchange is adopted, and it can be given as follows:

$$k_{TEG}\frac{\partial T_{TEG}}{\partial z} = h_{wind}(T_{amb} - T_{TEG}) \quad (13)$$

- **Heat transfer coefficients**

The heat transfer coefficient loss (h_{wind}) by convection to the surroundings depends directly on the wind velocity (v_{wind}). It can be expressed as follows:

$$h_{wind} = 5.82 + 4.07v_{wind} \quad (14)$$

The heat transfer coefficient loss (h_{rad}) by radiation to the sky is related to the emissivity of the cover, Stefan–Boltzmann constant, and the sky and glazing temperatures, respectively. It can be expressed as follows:

$$h_{rad} = \varepsilon_{glass}\sigma(T_g^2 + T_{sky}^2)(T_g + T_{sky}) \quad (15)$$

where the sky is considered as a black body and its temperature is related to the ambient temperature. The following expression can estimate it [20]:

$$T_{sky} = T_{amb} - 6 \quad (16)$$

2.2. Performance Expression

The electrical efficiency is provided by the polycrystalline silicon layer (η_{pv}), which is assumed to be zero for all the other layers (glass, above EVA, below EVA, and the Tedlar). It is related to its operating temperature and it can be calculated by the following equation [3]:

$$\eta_{pv} = \eta_{ref}[1 - \beta(T_c - T_{ref})] \quad (17)$$

where β is the polycrystalline silicon solar cell temperature coefficient, η_{ref} is the standard electrical conversion efficiency for a reference temperature (298.15 K), T_{pv} is the working polycrystalline silicon layer temperature.

The open circuit voltage is related to the Seebeck coefficient (α) and the difference temperature between the hot and cold side (ΔT) and the following expression can estimate it:

$$V_{OC} = \alpha\Delta T \quad (18)$$

The electrical output generated by the TE module is related to the load current (I) and the external load resistance ($R_{L)}$ and the following expression can calculate it [20]:

$$P_{teg} = (V_{OC} - R_{in})I = R_L I^2 = \frac{R_L \cdot \alpha^2 \cdot \Delta T^2}{(R_{in} + R_L)^2} \quad (19)$$

where R_{in} represents the internal load resistance.

The conversion efficiency of the TE module (η_{teg}) is expressed as:

$$\eta_{teg} = \frac{P_{teg}}{Q_h \times A_{te}} \quad (20)$$

Q_h is the input heat flux at the top surface of the TE (W/m^2), A_{te} (m^2) is the area of the TE top surface , P_{teg} is the TEG power output (W) and η_{teg} is the TEG efficiency (%).

The conversion efficiency of the CPV-TE (η_{cpv-te}) is defined as:

$$\eta_{cpv-te} = \eta_{pv} + \eta_{teg} \quad (21)$$

2.3. Computational Domain

The physical phenomena governing the behaviour of CPV-TE are numerous and complex. In this regard, an original multi-physics model is developed based on the coupling of radiative, conductive and convective transfers as well as the photovoltaic conversion and thermoelectric phenomena within such a CPV-TE system. In the present investigation, a computational commercial package COMSOL 5.4 Multiphysics software [26] was employed. The governing heat balance equations presented in the above sections were solved by the three-dimensional finite element method (FEM). The heat transfer in solid interface, electric current interface and electrical circuit interface were all used to perform the numerical investigation. The heat loss due to convection from the top surface of the PV glass layer is considered using boundary heat flux under heat transfer in solids. Furthermore, surface-to-ambient radiation is used to model the heat loss via radiation. Domain heat source is used to describe the energy absorbed in each layer of the photovoltaic and a temperature boundary condition is applied to the TEG cold surface to model the cooling. Furthermore, under the electric current interface, ground and terminal nodes are set to the negative and positive copper electrodes, respectively. In addition, an external load resistance is connected across both terminals under the electrical circuit interface. Thermoelectric effect is considered under the Multiphysics interface. A material is added to each component used this study under the material interface and the required material properties were inserted. Furthermore, the simulation process using COMSOL is shown in Fig. 2.

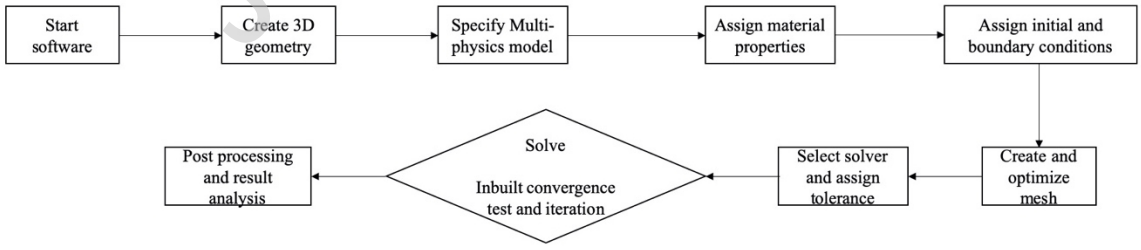

Figure 2: COMSOL simulation process.

2.4. Mesh independence test

To investigate the mesh test independence of the numerical model, a different type of meshing including 4390, 97935, 188937 and 591486 domain elements are tested (Table 3). In all these types of

meshing, the convergence is achieved. It is noted that from 188937 cells, no significant variation in CPV-TE electrical efficiency and solar cell temperature is observed. For this, 188937 numbers of domains elements (Fig. 3) are adopted throughout the simulation to save computation time compared to 591486 of elements.

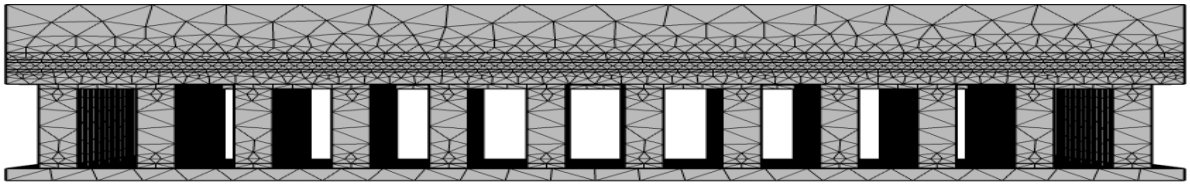

Figure 3: Front view of fine mesh employed in this study.

Table 3: Mesh convergence test.

Number of domain elements	Element size	Average cell temperature (K)	CPV-TE electrical efficiency (%)
4390	Coarser	360.85	14.3397
97935	Coarse	360.86	14.3387
188937	Normal	360.88	14.3369
591486	Fine	360.88	14.3369

2.5. Validation

The accuracy of the numerical model was verified by comparing the results of our simulations provided by COMSOL Multiphysics software with the previous works available in the literature [23,25]. To the author's knowledge, no experimental data are available for the integrated solar PV and TEG. The present numerical results were validated with previous modelling data available in the literature such as Zhou et al. [23] and Gao et al. [24]. The temperature distribution versus the thickness of the PV module for the present study was compared with the numerical study of Zhou et al. [23]. The comparison shows good agreement between the two studies. It is noted that the numerical results of Zhou et al. [23] were compared with the experimental study of Tina el al. [25] for solar PV module only using the same weather conditions (Irradiation = 800 W/m2, cell reference efficiency of 15%, and ambient temperature of 298 K). The results show a good agreement between the numerical (Zhou et al. [23]) and the experimental (Tina el al. [25]) data. Furthermore, for the TE model, the results of the proposed model (variation of TE efficiency against the Leg height – See Fig.4) was validated with the predicted results from Gao et al. [24]. A satisfactory agreement was also achieved. Therefore, the numerical results obtained in the course of this study are

accurate and justifiable and the proposed predictive model using the statistical analysis is reliable based on the proposed input factors.

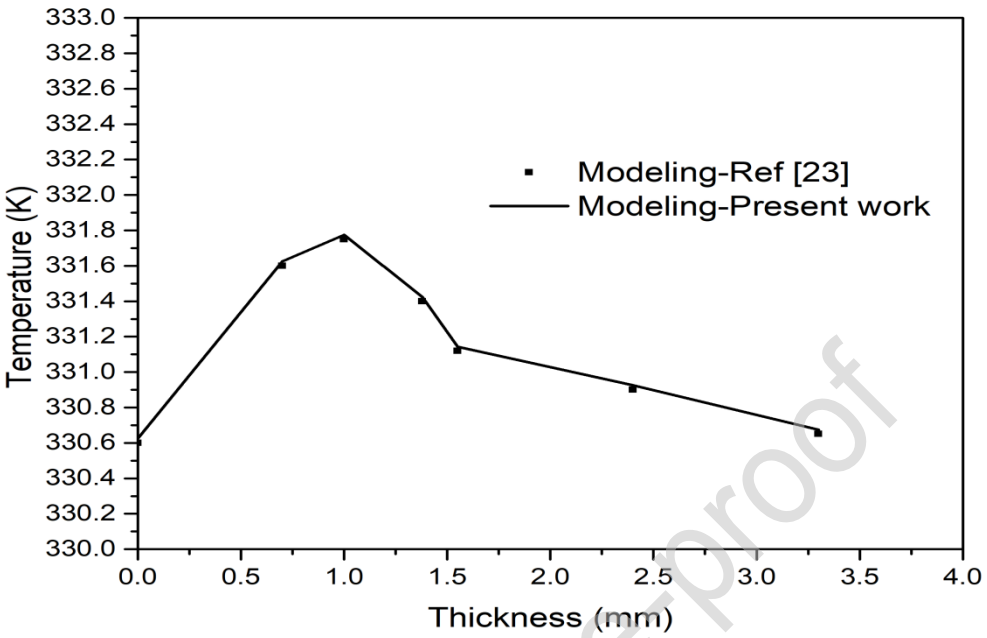

(b)

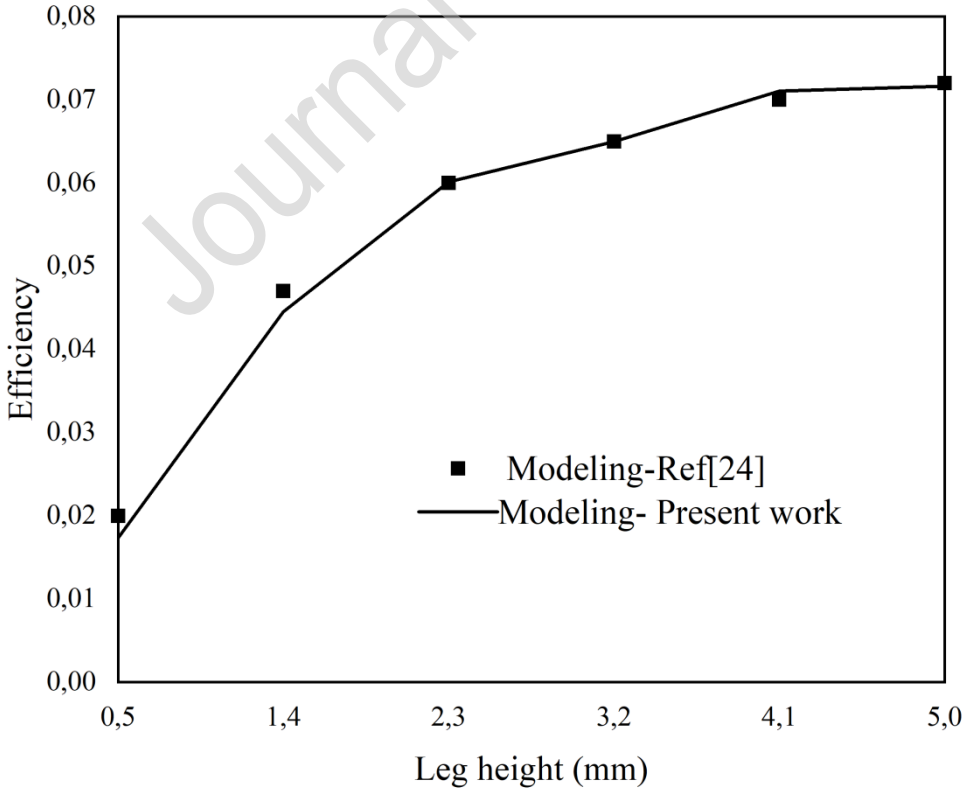

Figure 4: Validation of PV model with [23] and TEG model with [24].

2.6. Response surface methodology (RSM)

The response surface methodology (RSM) can be defined as a quantitative data of an experimental design suitable for determining and simultaneously solving the multivariate model. This model is a correlation between input variables (studied factors) and response surfaces. This model can be used to define the interrelations between the variables under test, and to describe the combined effects of all variables with a minimum number of real experiments.

To fit a relationship between the parameters and the responses through RSM. A quadratic regression model, which are determined corresponding to the 2nd-degree polynomial equation, is presented as follows:

$$y = \beta_0 + \sum_{i-1}^{n} \beta_i x_i + \sum_{i=1}^{n} \beta_{ii} x_i^{\,2} + \sum_{i=1}^{n-1} \sum_{j-i+1}^{n} \beta_{ij} x_i x_j \tag{22}$$

Where ε denotes the associated error term, β_i , β_{ii} , β_{ij} represent interactions coefficients of linear, second order and quadratic terms, respectively. y is the response of the model.

Equation 19 can be expressed for the quadratic regression model presented above in matrix arrangement by the following expression:

$$y = X\beta + \varepsilon \tag{23}$$

y is the vector of observations, X is the regressor matrix, β is the vector of the coefficients to be determined, and ε is the vector of errors. The least squares method is applied to estimate unknowns β and it can be expressed by the following expression:

$\beta = X^+ y$, where X^+ is the pseudo inverse of X and it is given as follows

$$X^+ = (X^T X)^{-1} X^T \tag{24}$$

The accuracy of the quadratic regression model is presented by the multiple determination coefficient (R^2) and the adjusted coefficient $\tilde{R}^2$.

The coefficient (R^2) represented the proportion of the model variability. A value close to 1 indicates the honesty of the model. The weakness of coefficient (R^2) doesn't consider the number of variables used to adjust the model. The following relation defines its expression:

$$R^2 = 1 - \frac{\sum_{i=1}^{n}(y_i - \tilde{y}_i)^2}{\sum_{i=1}^{n}(y_i - \overline{y}_i)^2} \quad (25)$$

$\tilde{R}^2$ is the adjusted coefficient of the regression model, it represents the correction of R^2, which takes into consideration the number of variables used in the model. The following relation defines its expression:

$$\tilde{R}^2 = 1 - (1 - R^2)\frac{n-1}{n-P-1} \quad (26)$$

Where $n - P - 1$ is the error of the degrees of freedom, and $n - 1$ is the total corrected degrees of freedom.

To understand the signification of the linear or interaction terms, a statistical tool (Fisher test) is performed, which consists of comparing the ratio between the variance of this term (AS_R) and the residual variance (AS_E) to that of a null rejection hypothesis ($F_{P,n-P-1,\sigma}$). If the F-value ($F = \frac{AS_R}{AS_E}$) is higher than the $F_{P,n-P-1,\sigma}$,the rejection of the null hypothesis is chosen, and then this term is statistically significant.

3. Application of Response Surface Methodology

In our present work, influence in order of importance of four parameters namely: the product of solar radiation and optical concentration, external load resistance, ambient temperature and height leg of TE, on the electrical efficiency of CPV-TE system is considered. As summarized in Table 4, the factorial part of CCD is a full factorial design with all combinations of the factors at two levels (maximum level, + 1 and minimum, − 1) and constituted of the 8-star points, and the 6 central points (0: middle level) which are the midpoint between the maximum and minimum levels. The star points are at the face of the cube part of the plan which represents α value of 1, and this type of plan is generally named the face-centred CCD. In this current work, a central composite design (CCD), with face central is selected, which for 30 runs numbers (Table 5) are required based on the following relation:

$$N = 2^{k} + 2k + n_c = 2^4 + 2.4 + 8 = 30$$

(27)

where N denotes the runs number, k represents the factors number, n_c is the number of replications at the central design point. Increasing the number of runs above 30, does not change the results.

Table 4: Range of selected input variables

Variables	**Levels**	
	-1	1
Solar radiation*optical concentration (W/m²)	200	10000
Ambient temperature (K)	298	318
Electrical load (Ω)	1.5	3.5
Leg height of TE module (mm)	0.5	5

Table 5: Actual values of independent variables along with their responses of electrical efficiency of CPV-TE system.

	Factor 1	**Factor 2**	**Factor 3**	**Factor 4**	**Response**
Run	**A: Solar radiation*optical concentration**	**B: Ambient temperature**	**C: Electrical load**	**D: Leg height of TE module**	**CPV-TE eff**
1	10000	318	1,5	0,5	15,49098
2	10000	298	1,5	5	12,31662
3	5100	308	2,5	2,75	15,8764
4	200	318	3,5	0,5	17,25051
5	200	318	1,5	5	17,06367
6	5100	308	2,5	2,75	15,8764
7	10000	318	1,5	5	12,1122
8	10000	318	3,5	5	13,00507
9	5100	318	2,5	2,75	15,81903
10	10000	318	3,5	0,5	15,28246
11	5100	308	3,5	2,75	15,95096
12	200	318	3,5	5	17,12791
13	5100	308	2,5	2,75	15,8764
14	5100	308	2,5	2,75	15,8764
15	200	318	1,5	0,5	17,26364
16	200	298	3,5	5	17,28302
17	200	298	1,5	5	17,2578

18	200	308	2,5	2,75	17,257
19	10000	298	1,5	0,5	15,56231
20	5100	298	2,5	2,75	15,93186
21	5100	308	2,5	0,5	16,35287
22	10000	308	2,5	2,75	14,44657
23	10000	298	3,5	5	13,18242
24	10000	298	3,5	0,5	15,3618
25	5100	308	2,5	2,75	15,8764
26	5100	308	2,5	5	15,02903
27	5100	308	2,5	2,75	15,8764
28	5100	308	1,5	2,75	15,70571
29	200	298	3,5	0,5	17,33055
30	200	298	1,5	0,5	17,33589

Table 6: Analysis of variance for of electrical efficiency of CPV-TE system.

Source	Sum of Squares	df	Mean Square	F-value	p-value	
Model	62,10	14	4,44	194,84	< 0.0001	significant
A-solar radiation*optical concentration	44,84	1	44,84	1969,52	< 0.0001	
B-Ambient temperature	0,0731	1	0,0731	3,21	0,0934	
C-External load resistance	0,1542	1	0,1542	6,77	0,0200	
D-leg height	9,18	1	9,18	403,14	< 0.0001	
AB	0,0001	1	0,0001	0,0026	0,9598	
AC	0,1022	1	0,1022	4,49	0,0512	
AD	7,07	1	7,07	310,38	< 0.0001	
BC	0,0002	1	0,0002	0,0069	0,9347	
BD	0,0115	1	0,0115	0,5030	0,4891	
CD	0,3237	1	0,3237	14,22	0,0019	
A^2	0,0009	1	0,0009	0,0389	0,8464	
B^2	0,0001	1	0,0001	0,0031	0,9566	
C^2	0,0046	1	0,0046	0,2001	0,6611	
D^2	0,0833	1	0,0833	3,66	0,0750	
Residual	0,3415	15	0,0228			
Lack of Fit	0,3415	10	0,0341			
Pure Error	0,0000	5	0,0000			

3.1. Analysis of variance (ANOVA)

The ability and denotation of the developed quadratic model by RMS is checked by analysis of variance (ANOVA). The moderate Fisher's (F-test) value is equal to 194.84, and the p-value of the model is very low (< 0.0001), which indicates that the quadratic model has a significant effect on the response. Besides the effect of linear factors (A: product of solar radiation and optical concentration, C: external load resistance load, and D: leg height of TE), interactions of variables (AD) and (CD) present the most important terms. As observed in Fig. 5, the comparison between the electrical efficiency of CPV-TE system provided by our developed model by COMSOL and the predicted results by the regression model confirms the closeness of predicted values to actual values. Moreover, as shown in Table 6, a 0.9583 value of "R-squared" and 0.9894 value of "Adjusted R-squared" were attained, (While the difference between "R-squared and "Adjusted R-squared" less than 0.2 is favourable) which explains an excellent match between the actual value provided by COMSOL and the fit of the regression equation developed. Sufficient precision for the electrical efficiency of the CPV/TE system is 48.389, (While values greater than 4 are suitable for the adequate accuracy), which demonstrates that the regression model can be employed to investigate the behaviour of our collector with good adequacy and reliability. Fig. 5 shows the comparison between the predicted results provided by RSM against the simulation of the electrical efficiency for CPV/TE system results provided by the numerical model. From this figure, a satisfactory range of errors between the actual and predicted values is obtained. A 0.9945 value of the determination coefficient (R^2) for the electrical efficiency was obtained. An excellent fitting was achieved between the forecast values obtained from the statistical model and the numerical data provided by the three-dimensional numerical model.

3.2. Model Estimation

The regression quadratic model for the electrical efficiency of the PV-TE response related to linear, interactions and quadratic terms can be expressed by the following correlation:

$$\eta_{PV-TE} = 15.87 - 1.58\mathrm{A} - 0.0637\mathrm{B} + 0.0925\mathrm{C} - 0.7141\mathrm{D} - 0.0019\mathrm{AB} + 0. + 0.0799\mathrm{AC} - 0.6646\mathrm{AD} + 0.0031\mathrm{BC} - 0.0268\mathrm{BD} + 0.1422\mathrm{CD} - 0.0185 A^2 + 0.0052B^2 - 0.0419C^2 - 0.1793D^2 \quad (28)$$

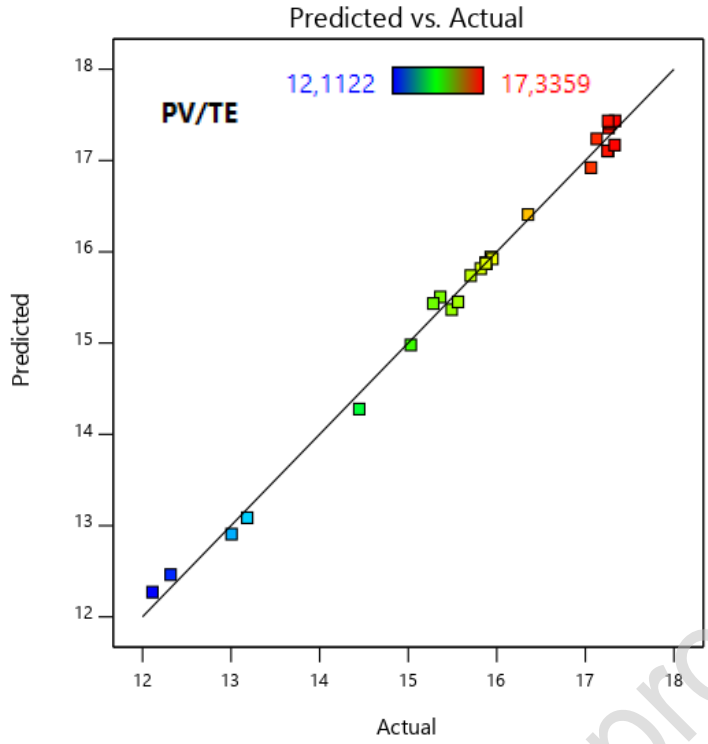

Figure 5: Comparison between the predicted results provided by RSM against simulation of the electrical efficiency of CPV/TE system.

4. Results and Discussions

4.1. Main Effects of Parameters on the Response

The influence of all input variables on the electrical efficiency of the CPV-TE system by the perturbation design is depicted in Fig. 6. The figure presents how the efficiency varies as each variable change from the determined reference point, with all other variables kept fixed at the reference value. In this figure, the slope of each factor line gives the sensitivity of the response to that factor. The electrical efficiency of the CPV-TE system is greatly affected by the concentration ratio and the solar radiation and the height TE legs as shown by the slope of the A and D lines. As illustrated in this figure, the rise of the concentration ratio and the solar radiation, the height TE legs and the ambient temperature cause a drop in electrical power output. Nevertheless, the increase in electrical resistance will enhance it. On the other hand, the effect of the parameters in order of importance on electrical efficiency is: product of solar radiation and optical concentration, the height of TE legs, external electrical resistance load, and ambient temperature.

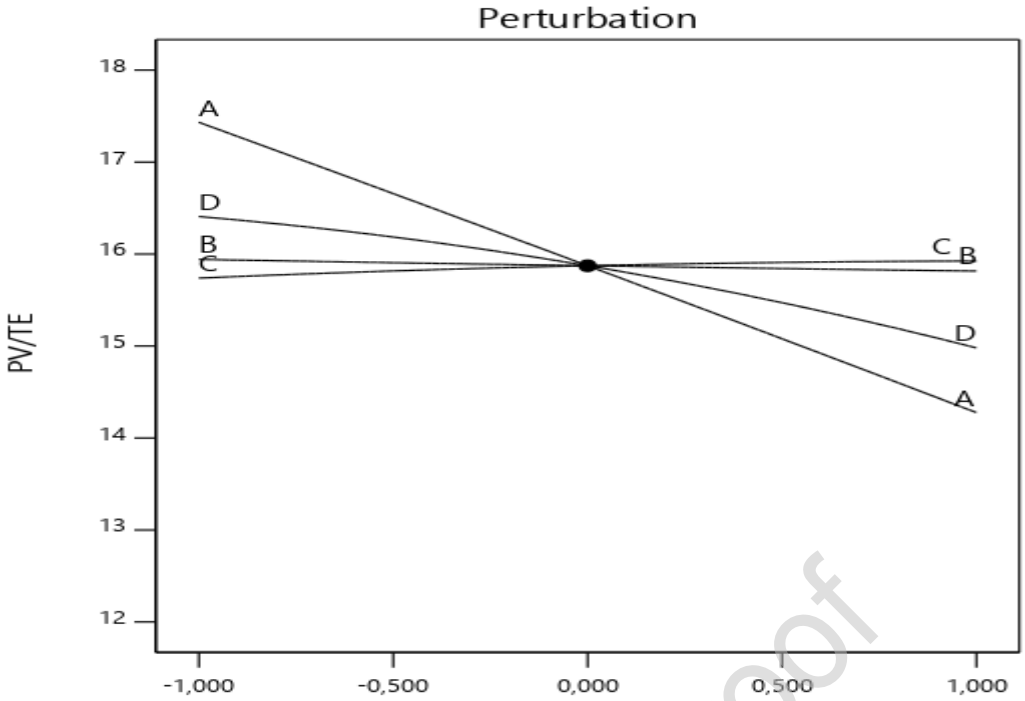

Fig. 6: Perturbation plot for the electrical efficiency of CPV-TE (A: product of solar radiation and optical concentration, B: ambient temperature, C: external electrical resistance load, D: the leg height of TE).

4.2. Binary Effects of Parameters on the Response

4.2.1. Effect of Solar Radiation and Ambient Temperature on the Electrical Efficiency of CPV-TE Hybrid System

The product of solar radiation and optical concentration, i.e. GC is varied from 200 W/m^2 to 10000 W/m^2 and the ambient temperature is varied from 298 K to 318 K, and the other parameters such as external electrical load resistance is fixed to 2.75 Ω and the leg height of the TE is fixed at 2.5 mm. Fig. 7 shows the variation of electrical efficiency of the CPV-TE system as a function of GC product and the ambient temperature. However, from Fig. 7, we can observe that the GC product plays a major role in affecting the electrical efficiency of PV-TE hybrid system than the ambient temperature. At the fixed ambient temperature of 318 K, the electrical efficiency of the hybrid system decreases from 17.27 % to 15.44 % as the GC product increases from 200 to 10,000 W/m^2. On the other hand, increasing the solar radiation leads to an increase in operating temperature of the PV module and therefore, the electrical efficiency decreases. The heat of the PV module is conducted from its backside to the hot side of the thermoelectric, which results in increased temperature between the hot and cold side of the TE module. Consequently, the electrical efficiency of the TE module is increased.

However, the scale of electrical efficiency of PV is higher than that of the TE module therefore, the efficiency of the CPV-TE system decreases. Besides, as presented in Fig. 7, the efficiency of the CPV-TE hybrid system drops with the increasing ambient temperature. At CG value of 10000 W/m^2, the efficiency of CPV-TE hybrid system decreases from 15.52 % to 15.44 % as the ambient temperature increases from 298 K to 318 K. The increased ambient temperature increases the operating temperature of the PV module. The rise in the temperature of the solar cell has a negative effect on its electrical efficiency. The PV module transfers its waste heat to the hot side of the TE module, which causes the increase in the TE module temperature. Consequently, the temperature difference between the hot side and the cold side of the TE module increases, and therefore, the enhancement in the electrical efficiency of the TE module occurs.

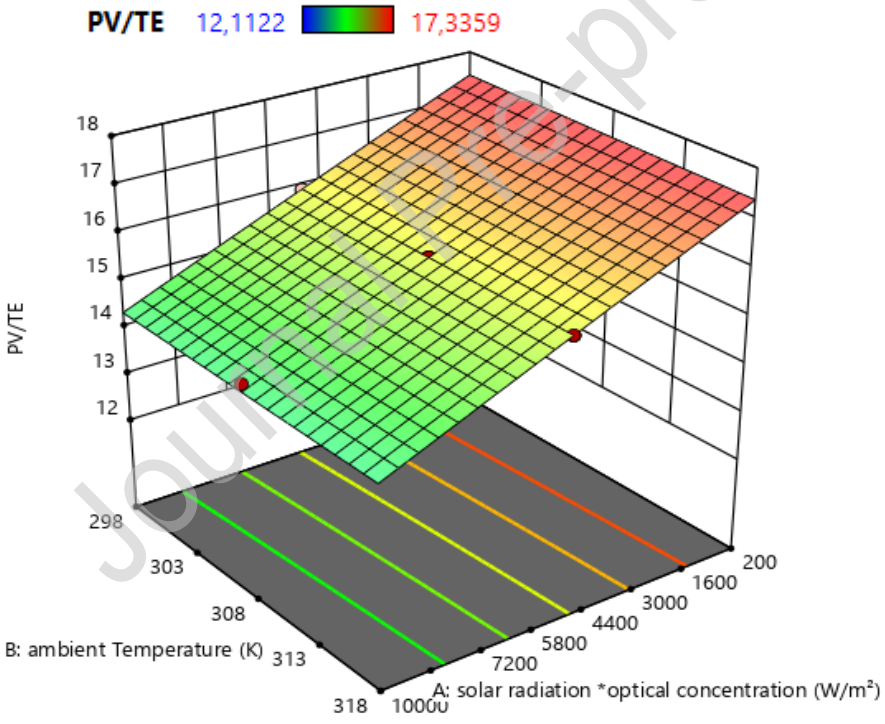

Figure 7:3D response surface plot illustrating interaction effects solar radiation and optical concentration (CG) and ambient temperature on the electrical CPV-TE system.

4.2.2. Influence of Amount of Solar Radiation and Optical Concentration (CG) and Load Resistance

The effect of the CG product and the load resistance on the electrical efficiency of the CPV-TE hybrid system at fixed ambient temperature of 308 K and fixed leg height of 2.5 mm, is shown in Fig. 8. It can be observed from Fig. 8 that the CG product plays the major role in affecting the electrical efficiency of the CPV-TE hybrid system as compared to the load resistance. For the fixed external load resistance of 2.5 Ω, the electrical efficiency of the CPV-TE hybrid system decreases from 17.34 % to 15.52 % when the GC product increases from 200 to 10000 W/m^2. On the other hand, for a 10000 W/m^2 value of the CG, when the external load resistance increases from 1.5 Ω to 3.5 Ω, a decrease in electrical efficiency of CPV-TE from 17.4344 % to 17.1689 % is obtained. Furthermore, the heat transfer in the TE module depends on the Peltier effect of the thermocouples and heat conduction. An increment in external load resistance leads to a reduction in electrical current of TE module which causes a rise in the temperature gradient between the hot and cold junctions of the TE module due to lower Peltier effect. The optimum electrical efficiency CPV-TE module is 17.3 % when the external load resistance is 2.8 Ω.

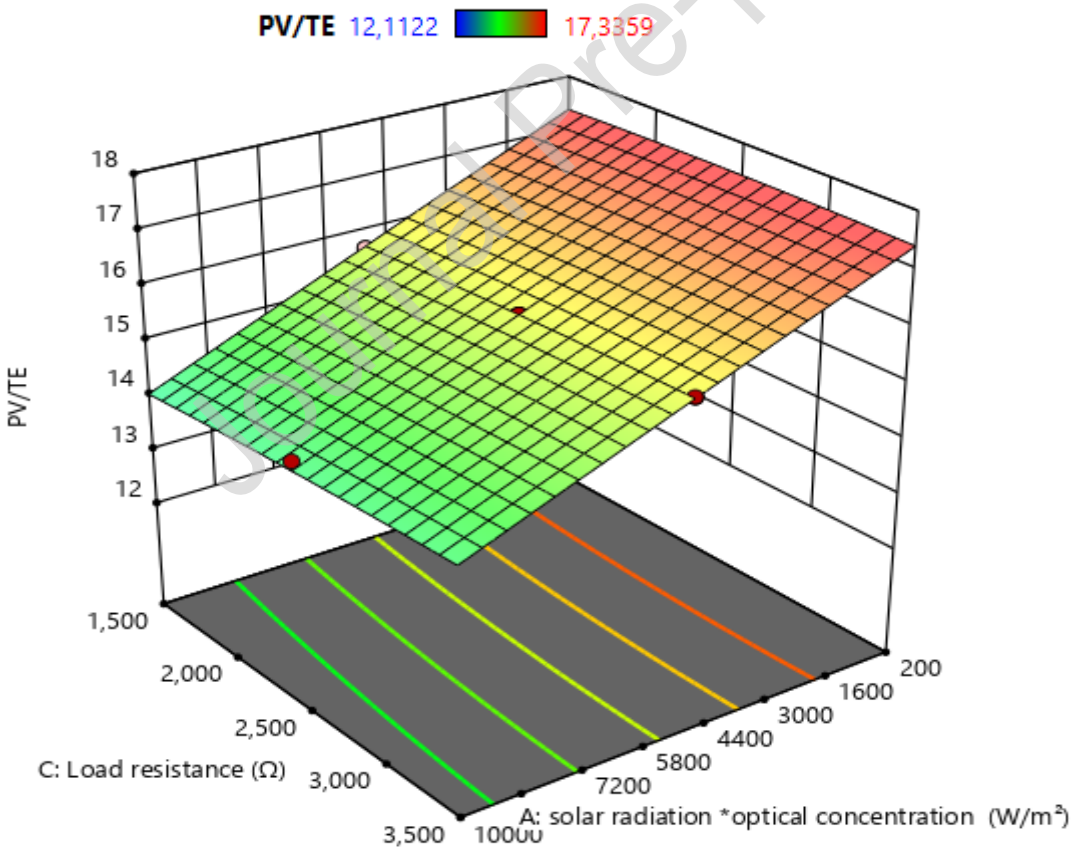

Figure 8:3D response surface plot illustrating interaction effects solar radiation and optical concentration (CG) and load resistance on the electrical CPV-TE.

4.2.3. Influence of Solar Radiation and Height of Legs of TE module

The combined effect of CG and leg height of TE modules on electrical efficiency of CPV-TE at ambient temperature of 308 K and external load resistance of 2.8 Ω is shown in Fig. 9. From this figure, we can note that, compared with the load resistance, CG plays the major role in affecting the electrical efficiency of CPV-TE system. For 2.75 mm value of height of legs of TE module, when the GC increases from 200 W/m^2 to 10000 W/m^2, a reduction in electrical efficiency of CPV-TE from 17.5001 % to 14.3474 % is obtained. On the other hand, for 10000 W/m^2 value of the CG, when the height of legs of TE modules increases from 0.5 mm to 5 mm, a reduction in electrical efficiency of CPV-TE system from the 15.5199 % to 12.8162 % is obtained. On the other hand, the reduction of leg height leads to enhancement of the conductive conductance transfer between the PV module and the hot side of the thermoelectric, and this phenomenon causes a more extended gradient temperature between hot and cold junctions of P/N legs. Consequently, an improvement in electrical efficiency of the TE module is obtained. On the other hand, the leg height is related to the internal resistance, resistivity, and the leg cross sectional area therefore, an increase of leg height leads to increase of the internal resistance. However, a reduction of leg height leads to the enhancement in gradient temperature between the PV module and the hot side and then between the hot side and the cold side, which results in improvement an electrical efficiency of the thermoelectric module.

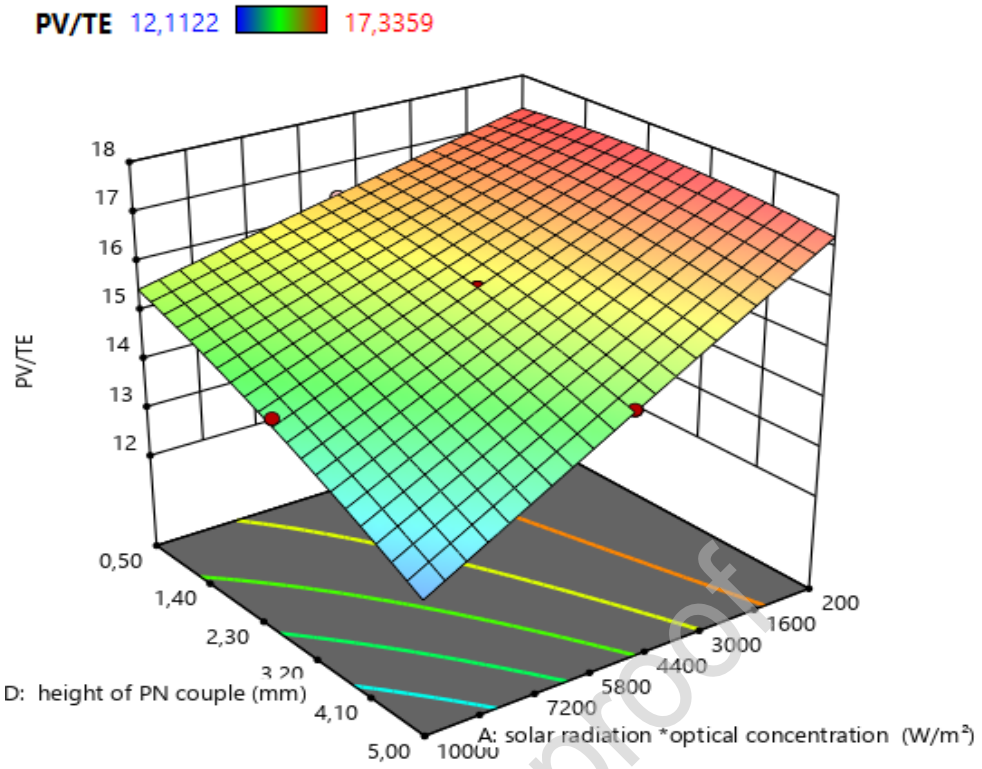

Figure 9:3D response surface plot illustrating interaction effects solar radiation and optical concentration (CG) height of PN couple on the electrical CPV-TE.

4.3. Optimization of designing parameters

One of the most helpful aims of RSM is determining an optimum response. In examining the selected response, the desirability changed from 0 to 1. Value of one describes the perfect optimized response, while zero shows that the predicted ideal response has lower quality. To test the desired response, the product of solar radiation and optical concentration, external load resistance, leg height of TE and ambient temperature were fixed to be in the selected range. In contrast, the electrical efficiency of CPV-TE system was maximum. The maximum electrical efficiency of the proposed CPVTE (17.448%) is obtained for optimum operating parameters at 229.698 W/m² value of Solar radiation x optical concentration, 303.353 K value of ambient temperature, 2.681Ω value of resistance electrical load and at 3.083 mm value of height of TE module.

Table 7: Range of input parameters and responses for optimization.

	Goal	Lower Limit	Upper Limit

A:Solar radiation x optical concentration	is in range	200	10000
B:Ambient temperature	is in range	298	318
C:Electrical load	is in range	1.5	3.5
D:Leg height of TE module	is in range	0.5	5
CPV-TE eff	maximize	12.1122	17.448

Conclusion

A numerical investigation is conducted in this work to examine the effect of four key parameters, i.e., the product of solar radiation and optical concentration, the external load resistance, the ambient temperature, and the leg height of TE on the efficiency of the hybrid CPV-TE system. Based on the numerical results, a polynomial statistical model was presented to forecast the electrical efficiency of CPV-TE system. The interactions between the studied input factors and their combined impact on the electrical efficiency are performed using a statistical RSM methodology. The Analysis of variance is conducted to investigate the significance of the proposed regression model. The key findings are:

- The determination coefficient (R^2) obtained for electrical efficiency is 0.9945. An excellent fitting is achieved between forecast values obtained from the statistical model and the numerical data provided by the three-dimensional numerical model.
- The influence of the parameters in order of importance on the electrical efficiency are respectively: product of solar radiation and optical concentration, the leg height of TE, external electrical resistance load, and ambient temperature.
- The simple quadratic statistical model can be employed to forecast and find the optimum hybrid system geometry and operating conditions to optimize the performance of CPV-TE.

- The maximum electrical efficiency of the proposed CPVTE (17.448%) is obtained for optimum operating parameters at 229.698 W/m² value of product of solar radiation and optical concentration, 303.353 K value of ambient temperature, 2.681Ω value of resistance electrical load and at 3.083 mm value of height of TE module.

ACKNOWLEDGMENT

The authors would like to thank Sharjah Electricity and Water Authority (SEWA), the Sustainable Energy Development Research Group, and the Research Institute for Science and Engineering at the University of Sharjah for the financial support - postdoctoral position at the University of Sharjah. Furthermore, this study was sponsored by the Project of EU Marie Curie International incoming Fellowships Program (745614).

Reference

[1] S. Shittu, G. Li, Y.G. Akhlaghi, X. Ma, X. Zhao, E. Ayodele, Advancements in thermoelectric generators for enhanced hybrid photovoltaic system performance, Renew. Sustain. Energy Rev. 109 (2019) 24–54. doi:10.1016/j.rser.2019.04.023.

[2] A. Abadeh, O. Rejeb, M. Sardarabadi, C. Menezo, M. Passandideh-Fard, A. Jemni, Economic and environmental analysis of using metal-oxides/water nanofluid in photovoltaic thermal systems (PVTs), Energy. 159 (2018) 1234–1243. doi:10.1016/j.energy.2018.06.089.

[3] O. Rejeb, H. Dhaou, A. Jemni, A numerical investigation of a photovoltaic thermal (PV/T) collector, Renew. Energy. 77 (2015) 43–50. doi:10.1016/j.renene.2014.12.012.

[4] O. Rejeb, M. Sardarabadi, C. Ménézo, M. Passandideh-Fard, M.H. Dhaou, A. Jemni, Numerical and model validation of uncovered nanofluid sheet and tube type photovoltaic thermal solar system, Energy Convers. Manag. 110 (2016) 367–377. doi:10.1016/j.enconman.2015.11.063.

[5] O. Rejeb, H. Dhaou, A. Jemni, Parameters effect analysis of a photovoltaic thermal collector: Case study for climatic conditions of Monastir, Tunisia, Energy Convers. Manag. 89 (2015) 409–419. doi:10.1016/j.enconman.2014.10.018.

[6] G. Li, S. Shittu, K. zhou, X. Zhao, X. Ma, Preliminary experiment on a novel photovoltaic-thermoelectric system in summer, Energy. 188 (2019) 116041. doi:https://doi.org/10.1016/j.energy.2019.116041.

[7] S. Shittu, G. Li, X. Zhao, X. Ma, Y.G. Akhlaghi, E. Ayodele, High performance and thermal

stress analysis of a segmented annular thermoelectric generator, Energy Convers. Manag. 184 (2019) 180–193. doi:10.1016/j.enconman.2019.01.064.

[8] Y.P. Zhou, M.J. Li, W.W. Yang, Y.L. He, The effect of the full-spectrum characteristics of nanostructure on the PV-TE hybrid system performances within multi-physics coupling process, Appl. Energy. 213 (2018) 169–178. doi:10.1016/j.apenergy.2018.01.027.

[9] G. Li, S. Shittu, T.M.O. Diallo, M. Yu, X. Zhao, J. Ji, A review of solar photovoltaic-thermoelectric hybrid system for electricity generation, Energy. 158 (2018) 41–58.

[10] W.G.J.H.M. Van Sark, Feasibility of photovoltaic - Thermoelectric hybrid modules, Appl. Energy. 88 (2011) 2785–2790. doi:10.1016/j.apenergy.2011.02.008.

[11] A. Lekbir, M. Meddad, E. A., S. Benhadouga, R. Khenfer, Higher-efficiency for combined photovoltaic-thermoelectric solar power generation, Int. J. Green Energy. 0 (2019) 1–7. doi:10.1080/15435075.2019.1567515.

[12] P.M. Rodrigo, A. Valera, E.F. Fernández, F.M. Almonacid, Performance and economic limits of passively cooled hybrid thermoelectric generator-concentrator photovoltaic modules, Appl. Energy. 238 (2019) 1150–1162. doi:10.1016/J.APENERGY.2019.01.132.

[13] B. Lorenzi, G. Chen, Theoretical efficiency of hybrid solar thermoelectric-photovoltaic generators, J. Appl. Phys. 124 (2018). doi:10.1063/1.5022569.

[14] D. Kraemer, L. Hu, A. Muto, X. Chen, G. Chen, M. Chiesa, Photovoltaic-thermoelectric hybrid systems: A general optimization methodology, Appl. Phys. Lett. 92 (2008). doi:10.1063/1.2947591.

[15] S. Shittu, G. Li, X. Zhao, X. Ma, Y.G. Akhlaghi, E. Ayodele, Optimized high performance thermoelectric generator with combined segmented and asymmetrical legs under pulsed heat input power, J. Power Sources. 428 (2019) 53–66. doi:10.1016/j.jpowsour.2019.04.099.

[16] S. Shittu, G. Li, X. Zhao, X. Ma, Series of detail comparison and optimization of thermoelectric element geometry considering the PV effect, Renew. Energy. 130 (2019) 930–942. doi:https://doi.org/10.1016/j.renene.2018.07.002.

[17] H. Hashim, J.J. Bomphrey, G. Min, Model for geometry optimisation of thermoelectric devices in a hybrid PV/TE system, Renew. Energy. 87 (2016) 458–463. doi:10.1016/j.renene.2015.10.029.

[18] G. Li, S. Shittu, X. Ma, X. Zhao, Comparative analysis of thermoelectric elements optimum geometry between Photovoltaic-thermoelectric and solar thermoelectric, Energy. 171 (2019) 599–610. doi:10.1016/j.energy.2019.01.057.

[19] P. Motiei, M. Yaghoubi, E. GoshtashbiRad, A. Vadiee, Two-dimensional unsteady state performance analysis of a hybrid photovoltaic-thermoelectric generator, Renew. Energy. 119 (2018) 551–565. doi:10.1016/j.renene.2017.11.092.

[20] S. Shittu, G. Li, X. Zhao, Y.G. Akhlaghi, X. Ma, M. Yu, Comparative study of a concentrated photovoltaic-thermoelectric system with and without flat plate heat pipe, Energy Convers. Manag. 193 (2019) 1–14. doi:10.1016/j.enconman.2019.04.055.

[21] S. Mahmoudinezhad, A. Rezania, L.A. Rosendahl, Behavior of hybrid concentrated photovoltaic-thermoelectric generator under variable solar radiation, Energy Convers. Manag. 164 (2018) 443–452. doi:10.1016/j.enconman.2018.03.025.

[22] European Thermodynamics Limited, GM250-127-14-16 Thermoelectric generator module - Datasheet, (2014) 1–4.

[23] J. Zhou, Q. Yi, Y. Wang, Z. Ye, Temperature distribution of photovoltaic module based on finite element simulation, Sol. Energy. 111 (2015) 97–103. doi:10.1016/j.solener.2014.10.040..

[24] J.-L. Gao, Q.-G. Du, X.-D. Zhang, X.-Q. Jiang, Thermal Stress Analysis and Structure Parameter Selection for a Bi2Te3-Based Thermoelectric Module, J. Electron. Mater. 40 (2011) 884–888. doi:10.1007/s11664-011-1611-3.

[25] Tina GM, Abate R. Experimental verification of thermal behaviour of photovoltaic modules. Proc. IEEE Mediterranean Electrotechnical Conf., Ajaccio, France; 2008, p.558-63.

[26] COMSOL Multiphysics® v. 5.4, www.comsol.com, COMSOL AB. Stockholm (2018) Sweden.

Author declaration

We wish to draw the attention of the Editor to the following facts, which may be considered as potential conflicts of interest, and to significant financial contributions to this work:

The nature of potential conflict of interest is described below:

☐No conflict of interest exists.

We wish to confirm that there are no known conflicts of interest associated with this publication and there has been no significant financial support for this work that could have influenced its outcome.

2. Funding

☐No funding was received for this work.

CRediT author statement

Manuscript title: « Optimization and analysis of a solar concentrated photovoltaic-thermoelectric (CPV-TE) hybrid system »

Oussama Rejeb: Conceptualization, Software, Validation, Writing - Original Draft.

Samson Shittu: Software, Validation, Writing - Original Draft

Chaouki Ghenai :Writing- Original draft preparation

Guiqiang Li : Writing- Reviewing and Editing

Xudong Zhao: Writing- Reviewing and Editing

Maamar Bettayeb: Writing- Reviewing and Editing

Highlights

- A three-dimensional Multiphysics model based on finite element method to investigate the performance of CPV-TE is presented.
- A quadratic model is developed to forecast the CPV-TE system electrical efficiency.
- The determination coefficient (R^2) obtained for electrical efficiency is 0.9945.
- The most influential parameters that affect the electrical efficiency are presented.
- The optimum parameters for the maximum efficiency of the CPV-TE are defined.